

Supplement of Weather Clim. Dynam., 4, 543–565, 2023
<https://doi.org/10.5194/wcd-4-543-2023-supplement>
© Author(s) 2023. CC BY 4.0 License.



Supplement of

Convection-parameterized and convection-permitting modelling of heavy precipitation in decadal simulations of the greater Alpine region with COSMO-CLM

Alberto Caldas-Alvarez et al.

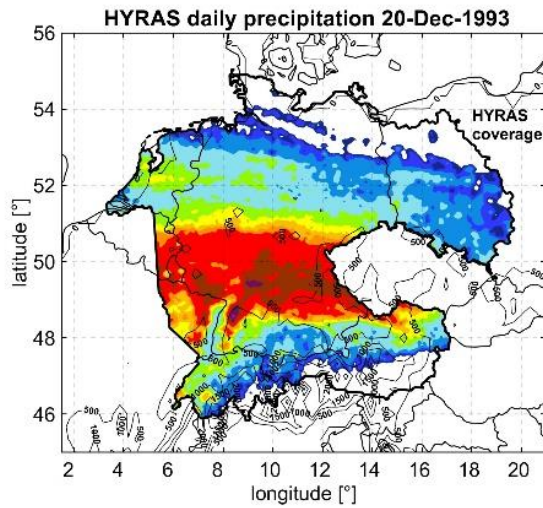
Correspondence to: Alberto Caldas-Alvarez (caldalv.alberto@gmail.com) and Hendrik Feldmann (hendrik.feldmann@kit.edu)

The copyright of individual parts of the supplement might differ from the article licence.

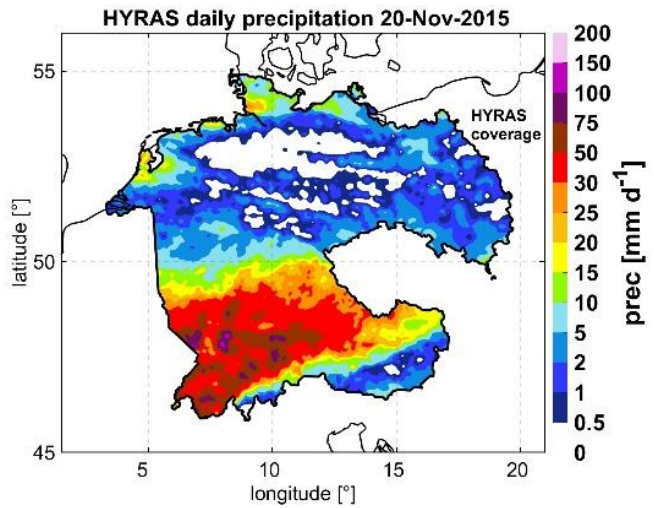
5 Supplement

Supplementary material

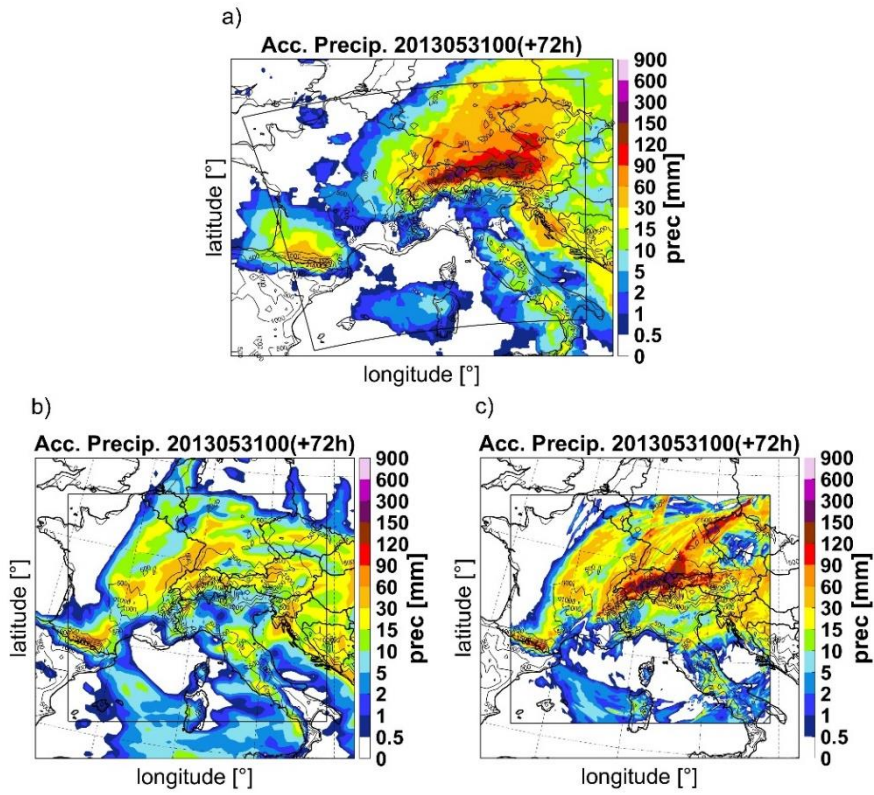
a)



b)

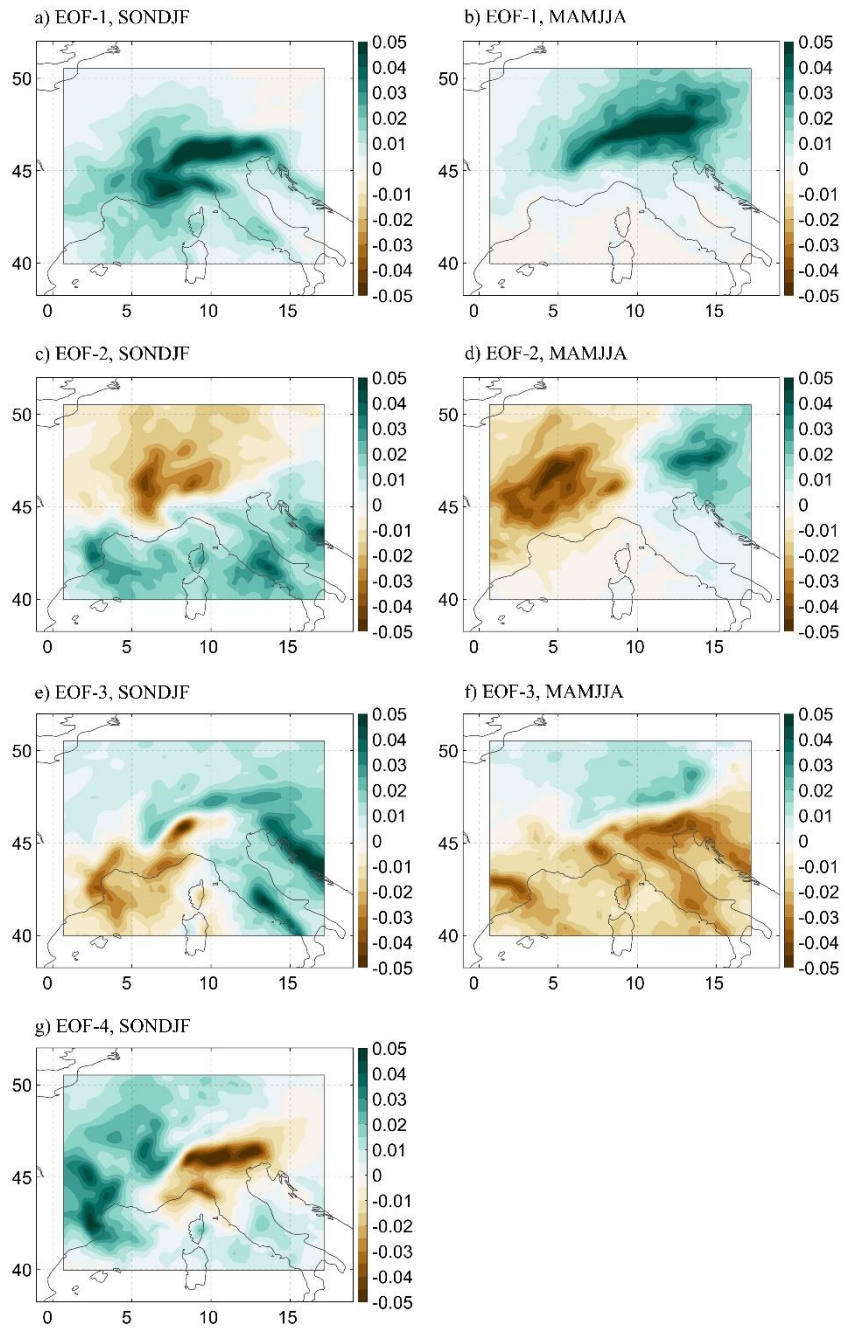


- 10 Figure S1. (a) Spatial distribution of the percentile-80 of precipitation climatology in the period 1975-2015 for HYRAS-5km. (b) Spatial distribution of daily precipitation during the 20-Dec-1993 and (c) the 20-Nov-2015.

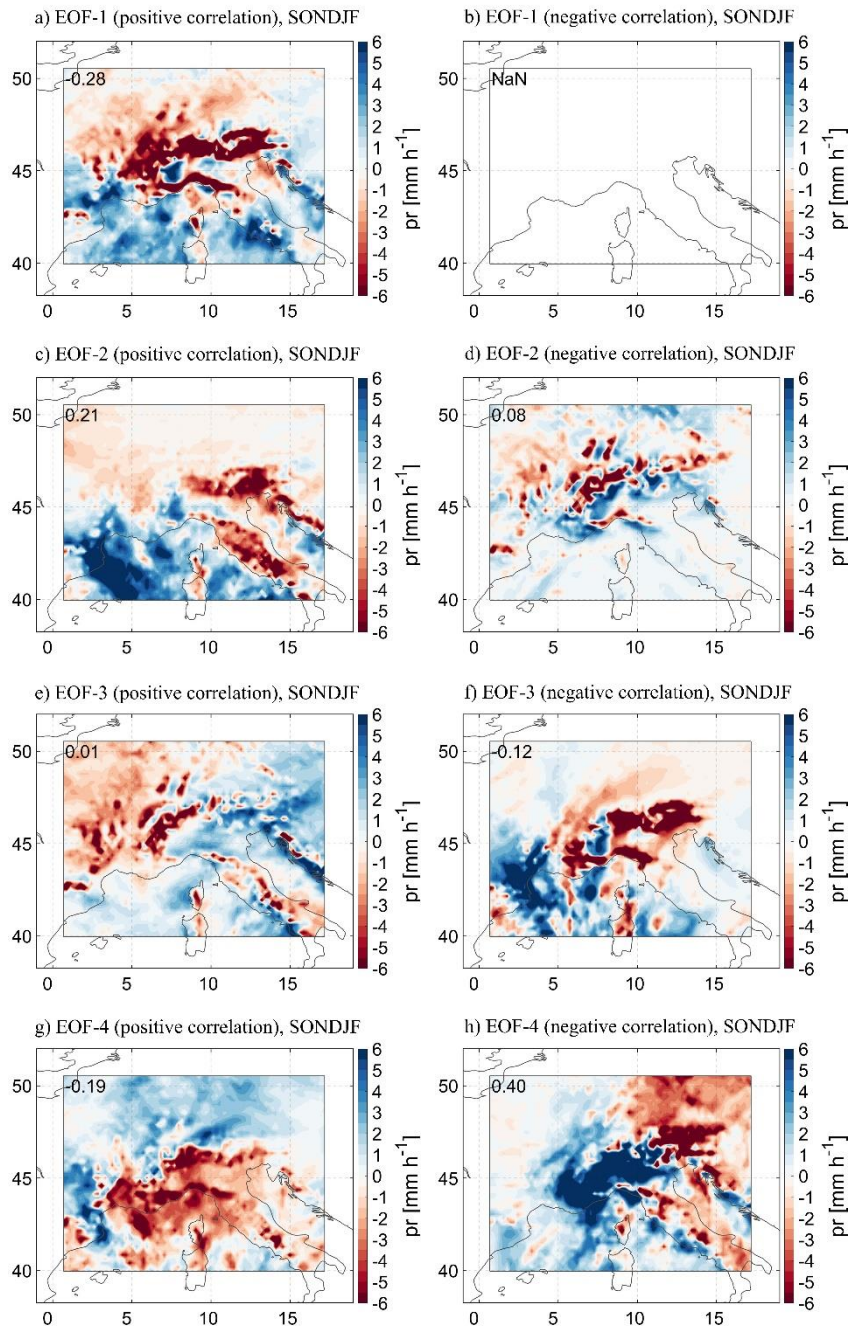


15

Figure S2. Spatial distribution of 72h accumulated precipitation for the event 31-May-2013 as observed by MSWEP-11km (a) and simulated by RCM (b) and CPM (c). The contours represent the surface height.



20 Fig. S3. As Fig. 9 but for RCM



25 **Figure S4. Composite precipitation differences between RCM (blue) and CPM (red). Composites derived using the heavy precipitation days with the largest positive and negative correlation with Winter (SONDJF) EOFs.**

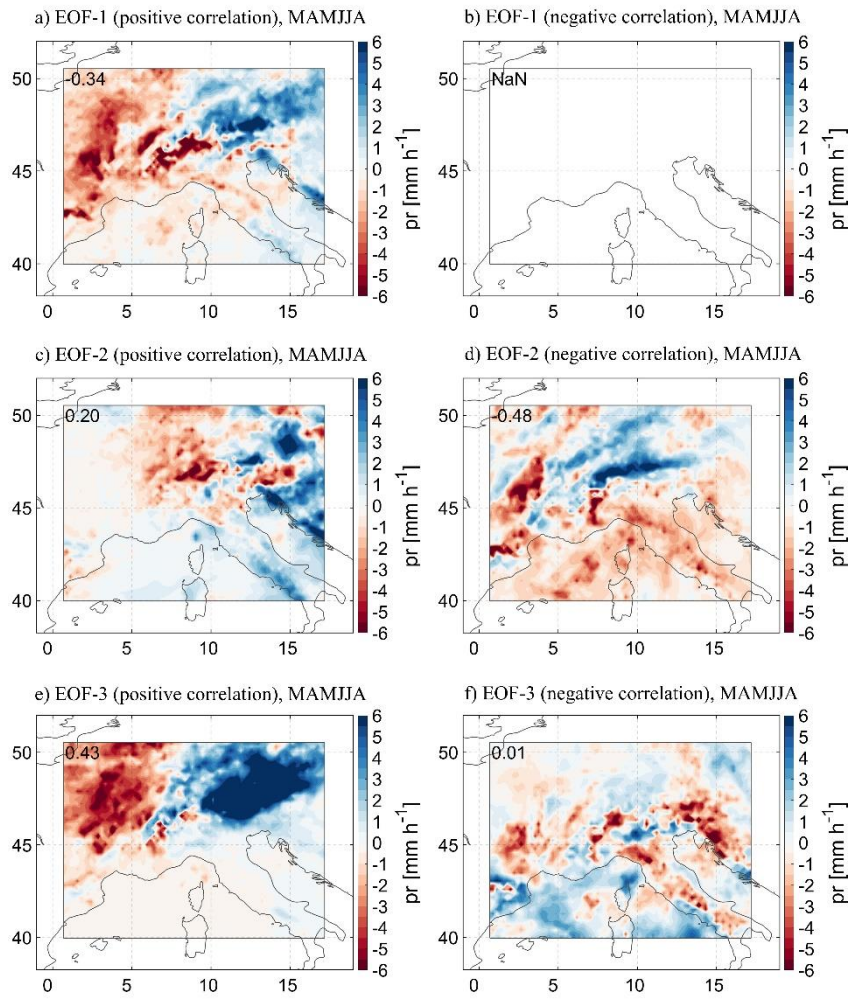


Figure S5. As Fig. S4 but for summer events (MAMJJA).

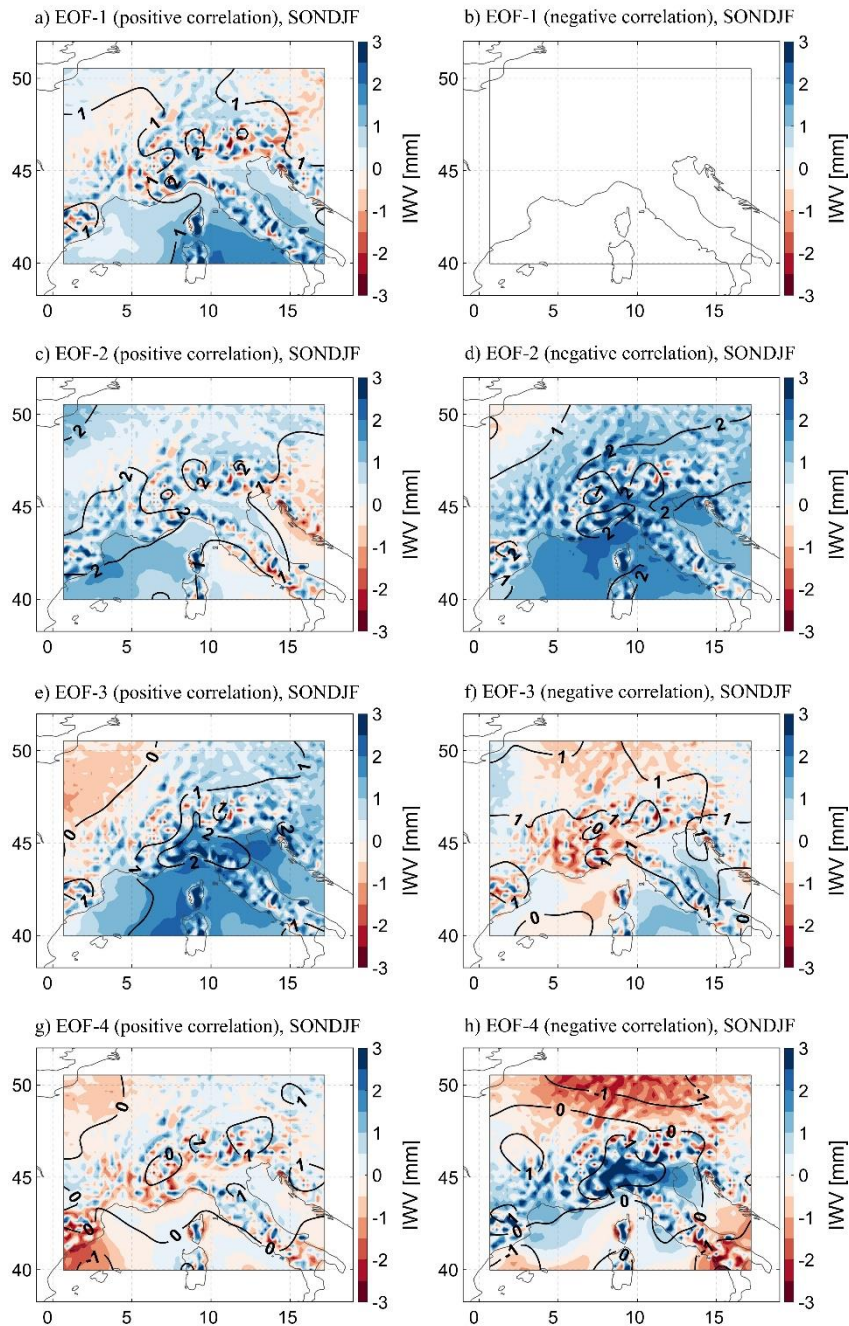


Figure S6. Composite IWV and θ_e^{850} differences between RCM (blue) and CPM (red). The θ_e^{850} differences are shown as contour levels in steps of 1 K. All composites derived using the heavy precipitation days with the largest positive and negative correlation with Winter (SONDJF) EOFs.

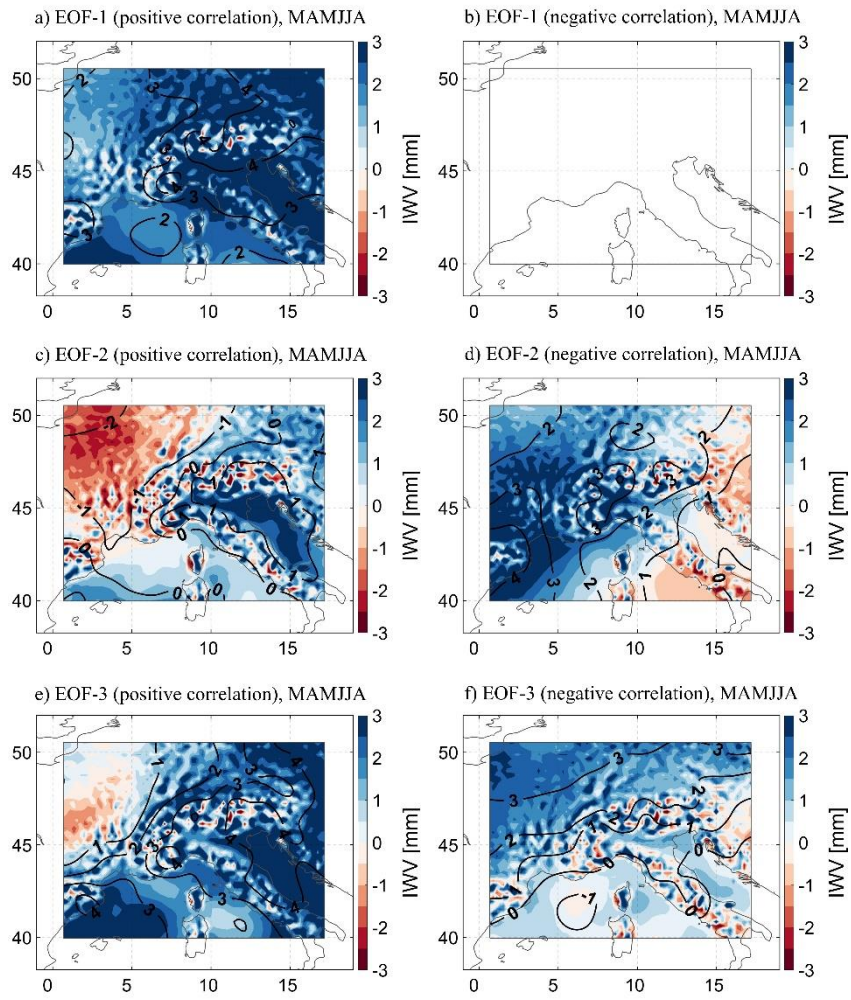
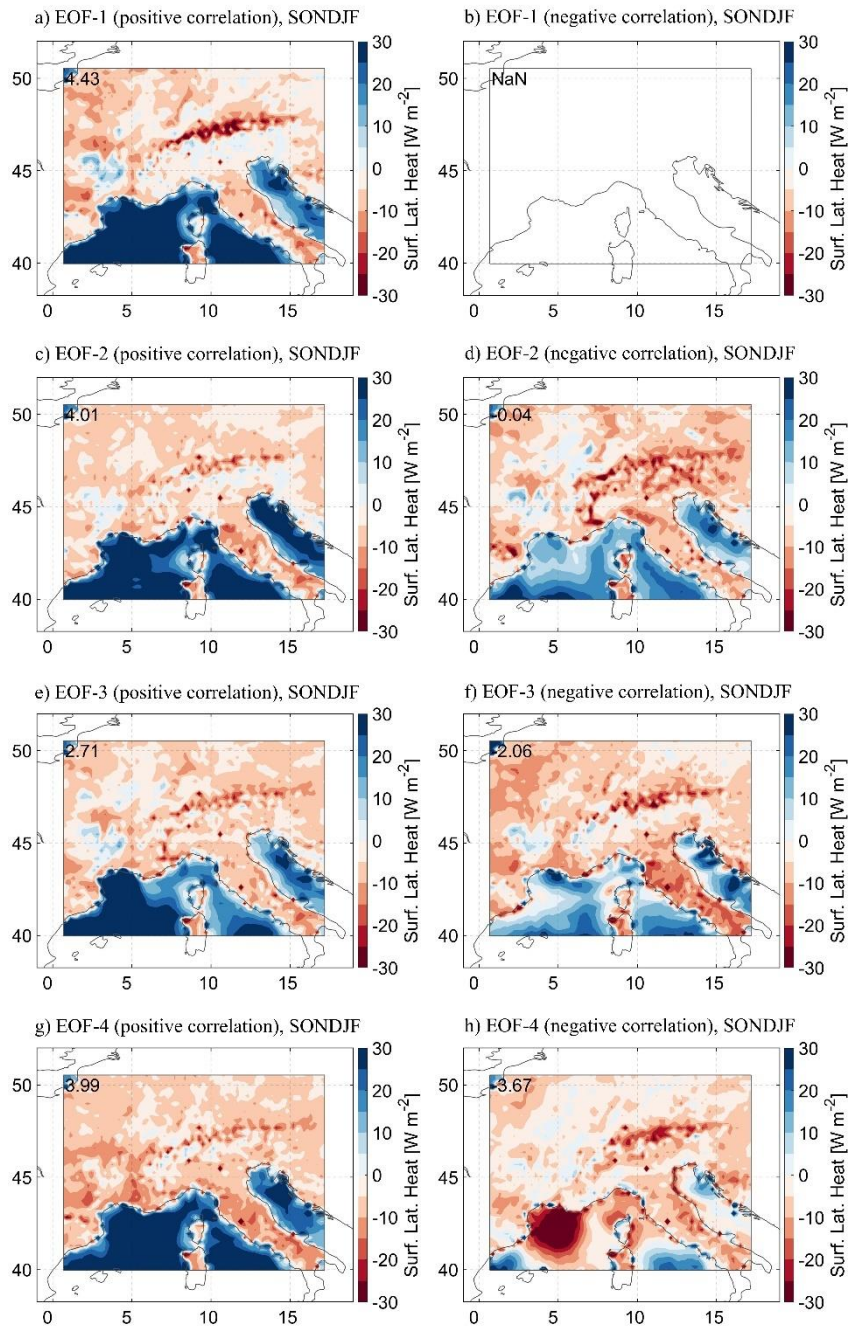
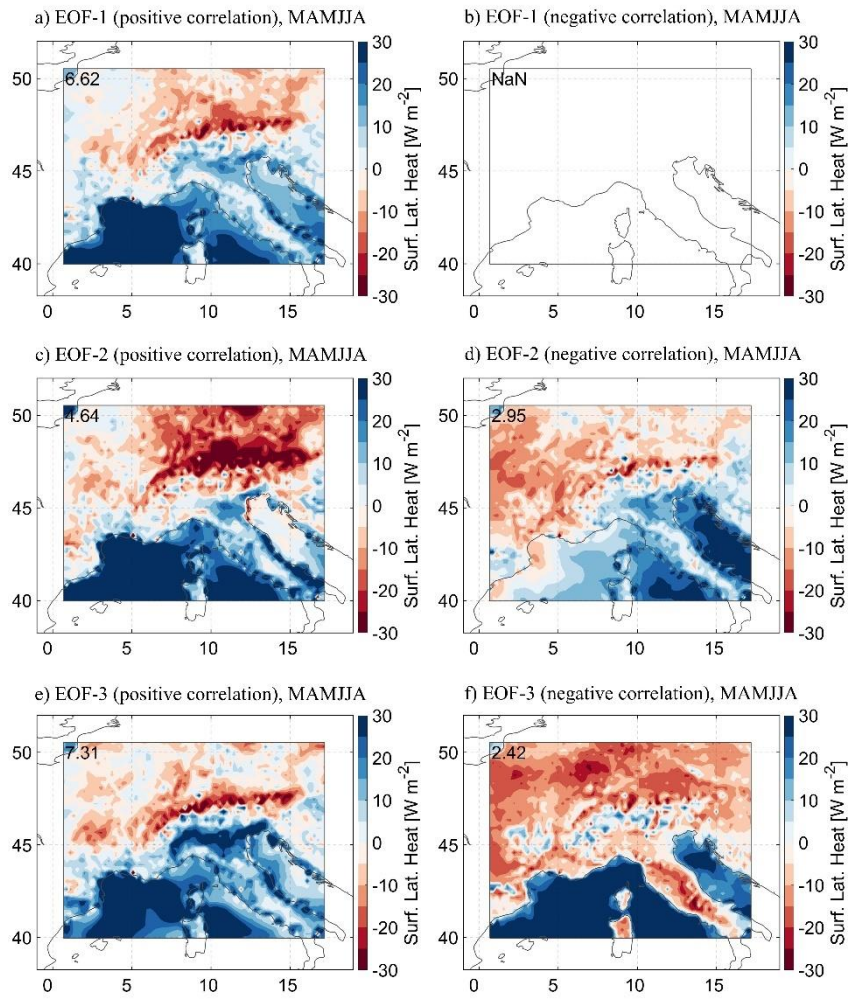


Figure S7. As Fig. S6 but for summer events (MAMJJA).



40 **Figure S8. Composite latent heat flux differences between RCM (blue) and CPM (red). All composites derived using the heavy precipitation days with the largest positive and negative correlation with Winter (SONDJF) EOFs.**



45 **Figure S9.** As Fig. S8 but for summer events (MAMJJA).

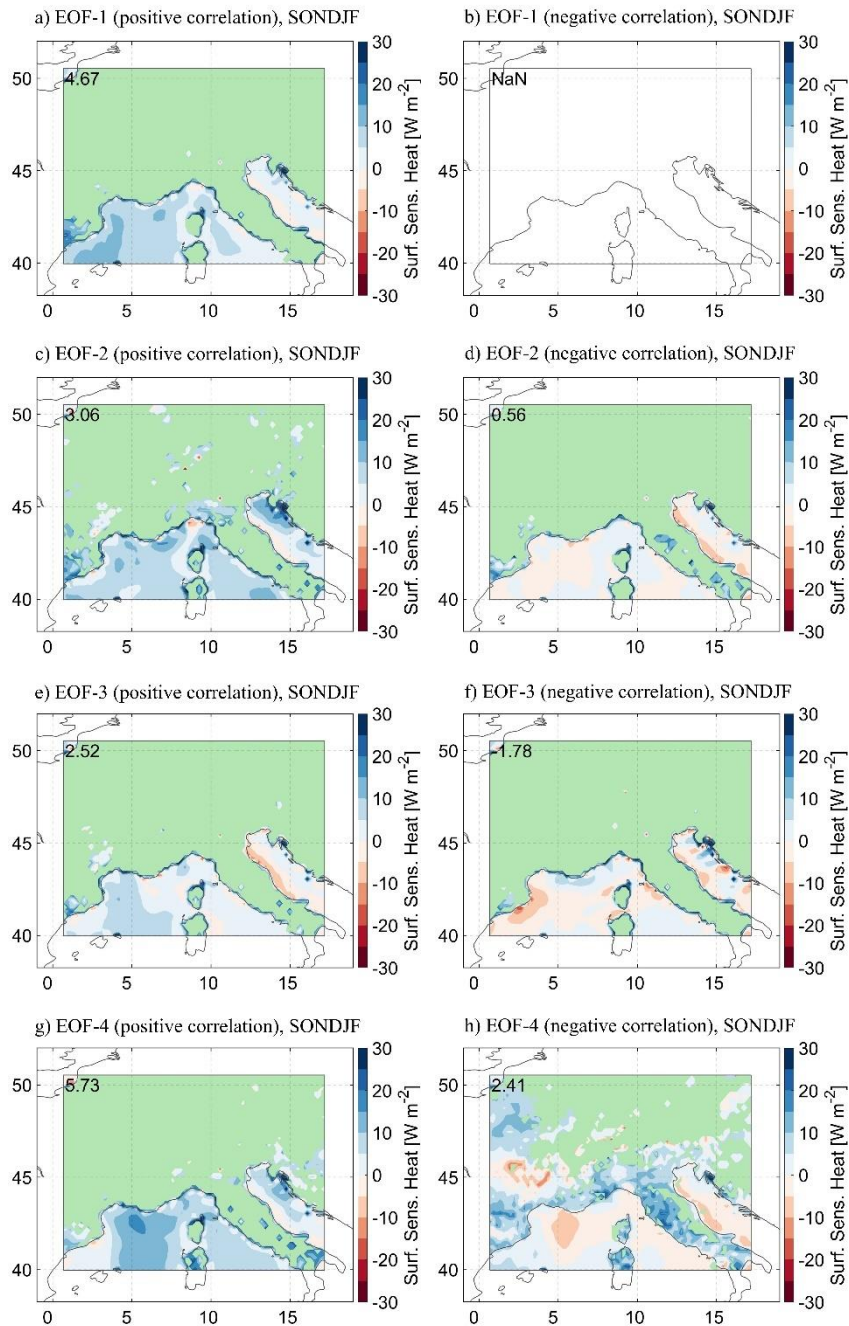


Figure S10. Composite sensible heat flux differences between RCM (blue) and CPM (red). Green areas denote no net outbound heat emissions. All composites derived using the heavy precipitation days with the largest positive and negative correlation with Winter (SONDJF) EOFs.

50

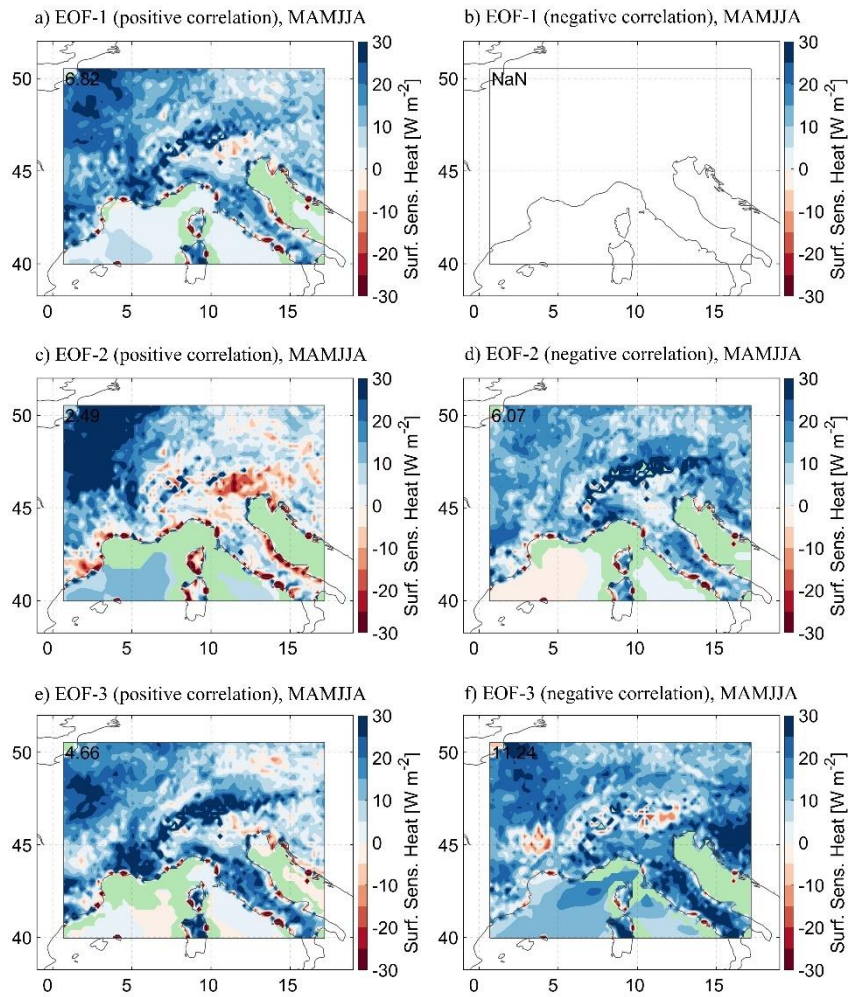


Figure S11. As Fig. S10 but for summer events (MAMJJA).

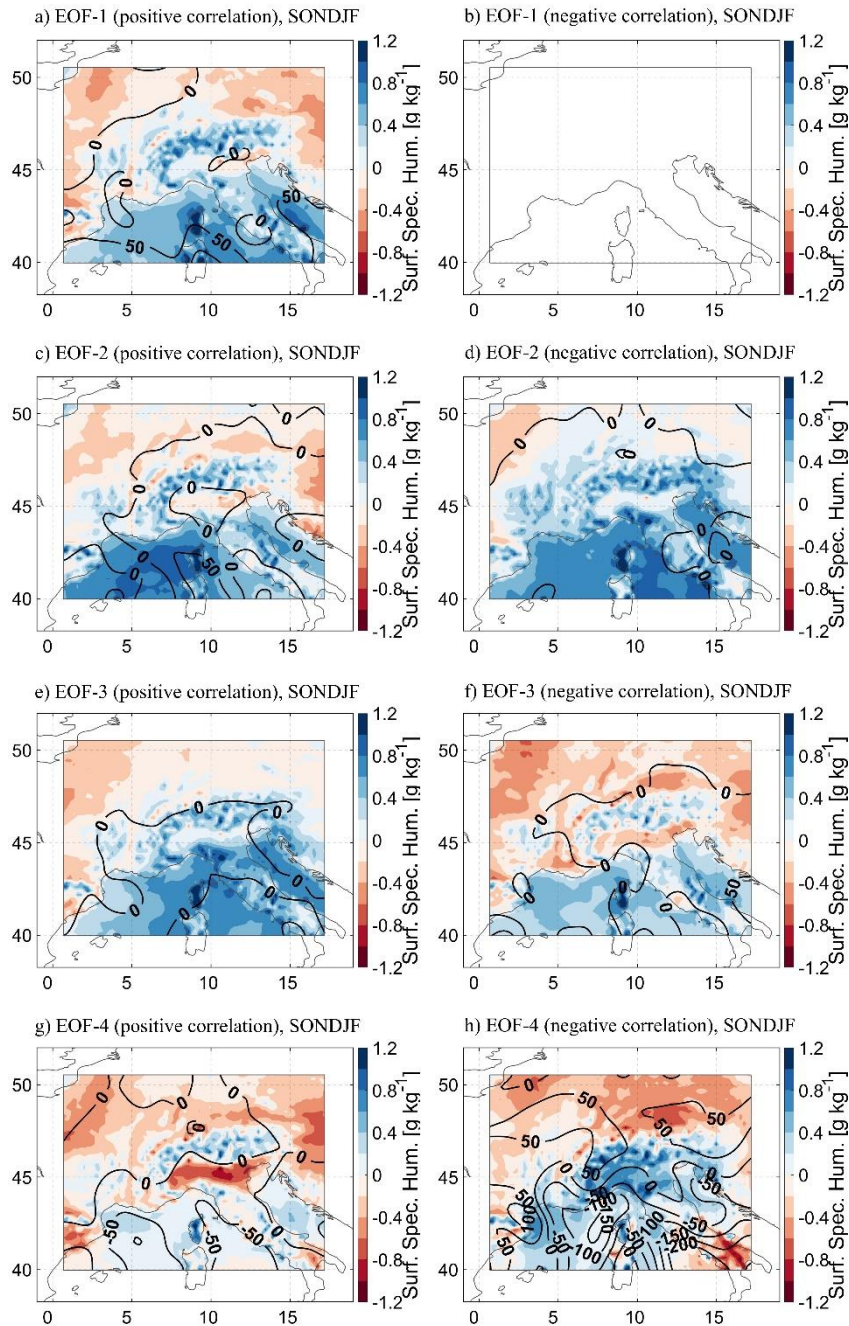


Figure S12. Composite surface specific humidity and CAPE differences between RCM (blue) and CPM (red). The CAPE differences are shown as contour levels in steps of 50 J Kg⁻¹. All composites derived using the heavy precipitation days with the largest positive and negative correlation with Winter (SONDJF) EOFs.

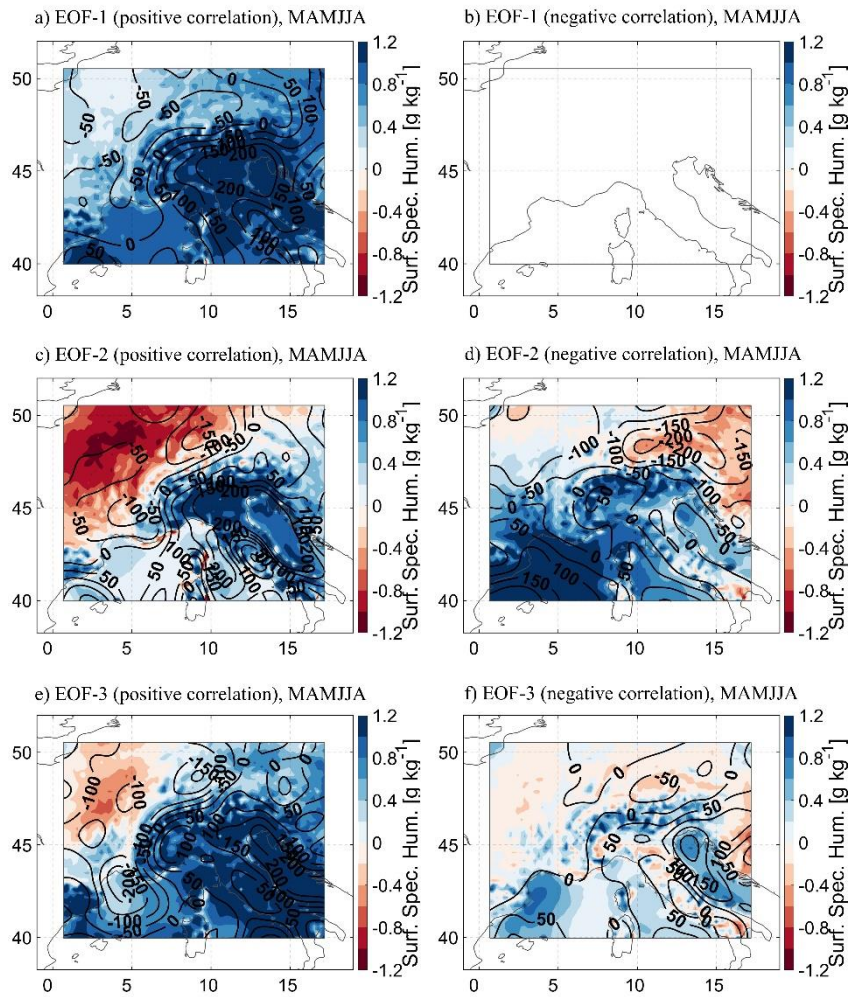
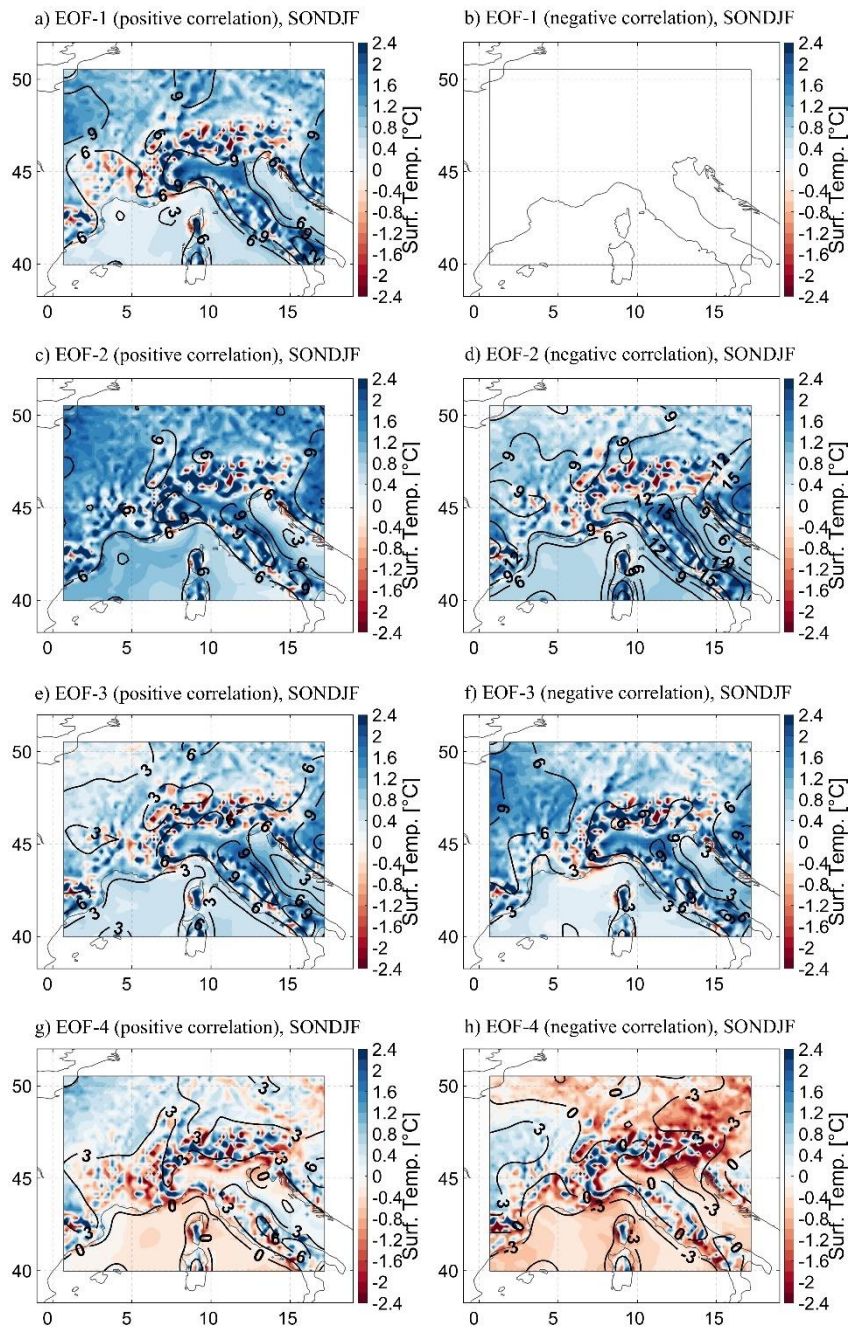
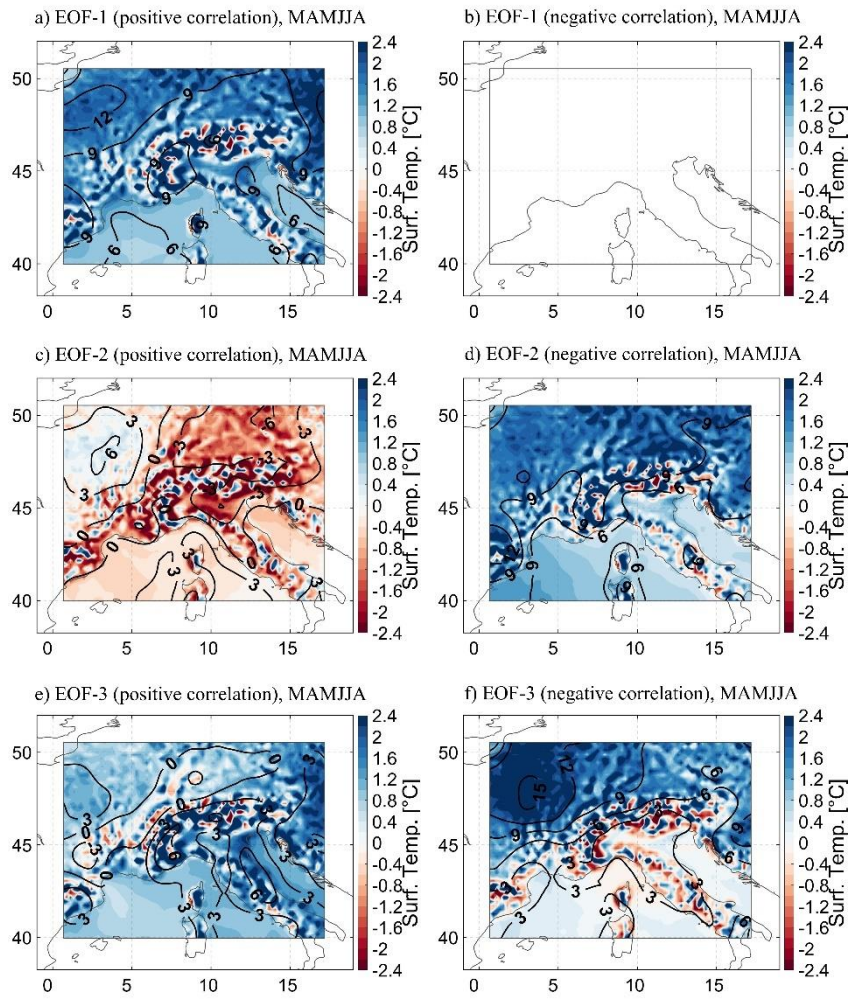


Figure S13. As Fig. S12 but for summer events (MAMJJA).



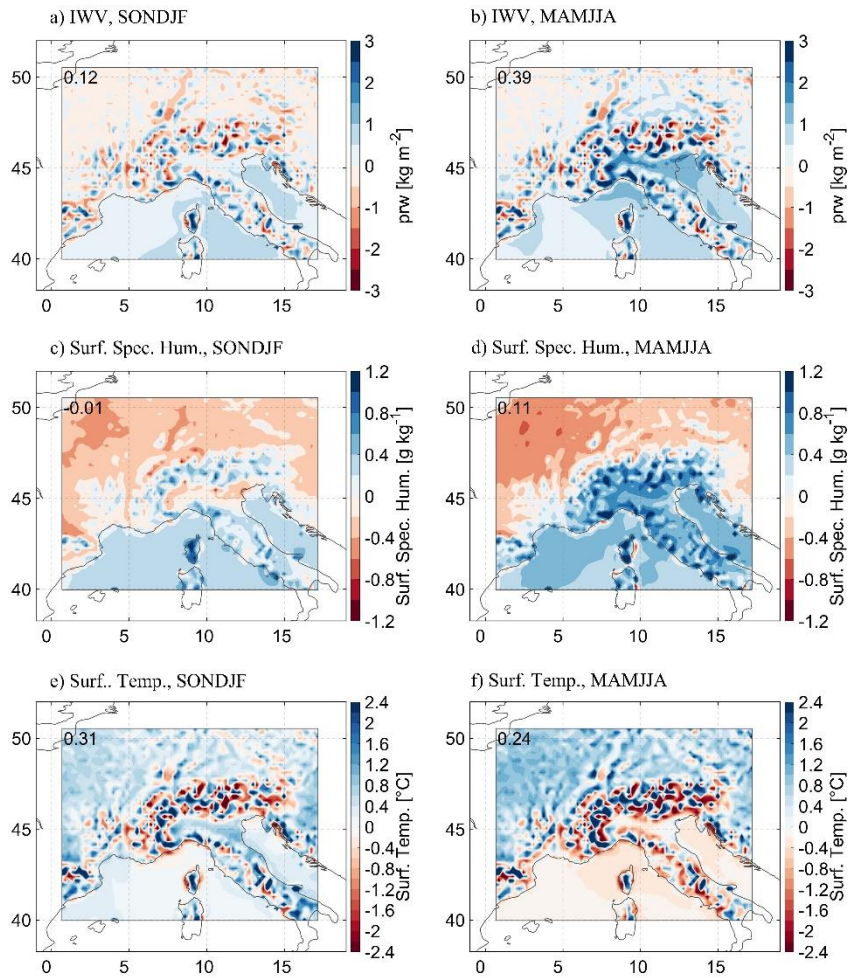
75

Figure S14. Composite surface temperature and outbound longwave radiation differences between RCM (blue) and CPM (red). The outbound longwave radiation differences are shown as contour levels in steps of 3 $W m^{-2}$. All composites derived using the heavy precipitation days with the largest positive and negative correlation with Winter (SONDJF) EOFs



80

Figure S15. As Fig. S14 but for summer events (MAMJJA).



85 **Figure S16. Differences between RCM (blue) and CPM (red) for the seasonal means of Integrated Water Vapour (a, b), surface specific humidity (c, d), and surface temperature (e, f).**

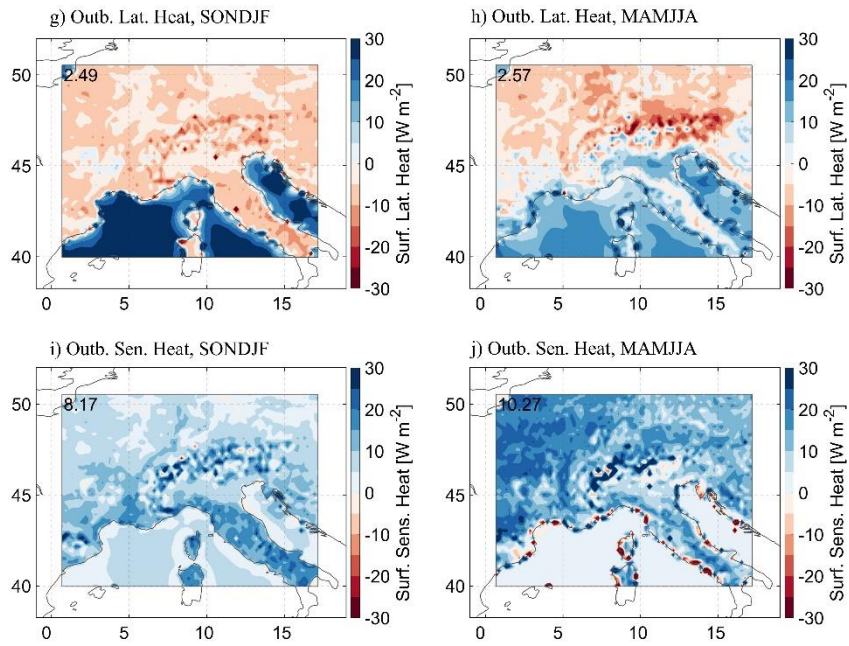


Figure S17. As Fig. S16 but for outbound latent heat fluxes (a, b) and outbound sensible heat fluxes (c, d).